Electronic Supplementary Material (ESI) for CrystEngComm

Supporting Information

Micro and Nanosized Architectures in Hydrothermal Tm^{3+}-Doped $GdVO_4$: Chemical Insights Towards Preservation of the 2 μm Emission Efficiency

Rocío Calderón-Villajos, Carlos Zaldo and Concepción Cascales*

* (e-mail ccascales@icmm.csic.es)

Instituto de Ciencia de Materiales de Madrid, Consejo Superior de Investigaciones Científicas CSIC, c/Sor Juana Inés de la Cruz, 3, E-28049 Madrid, Spain.

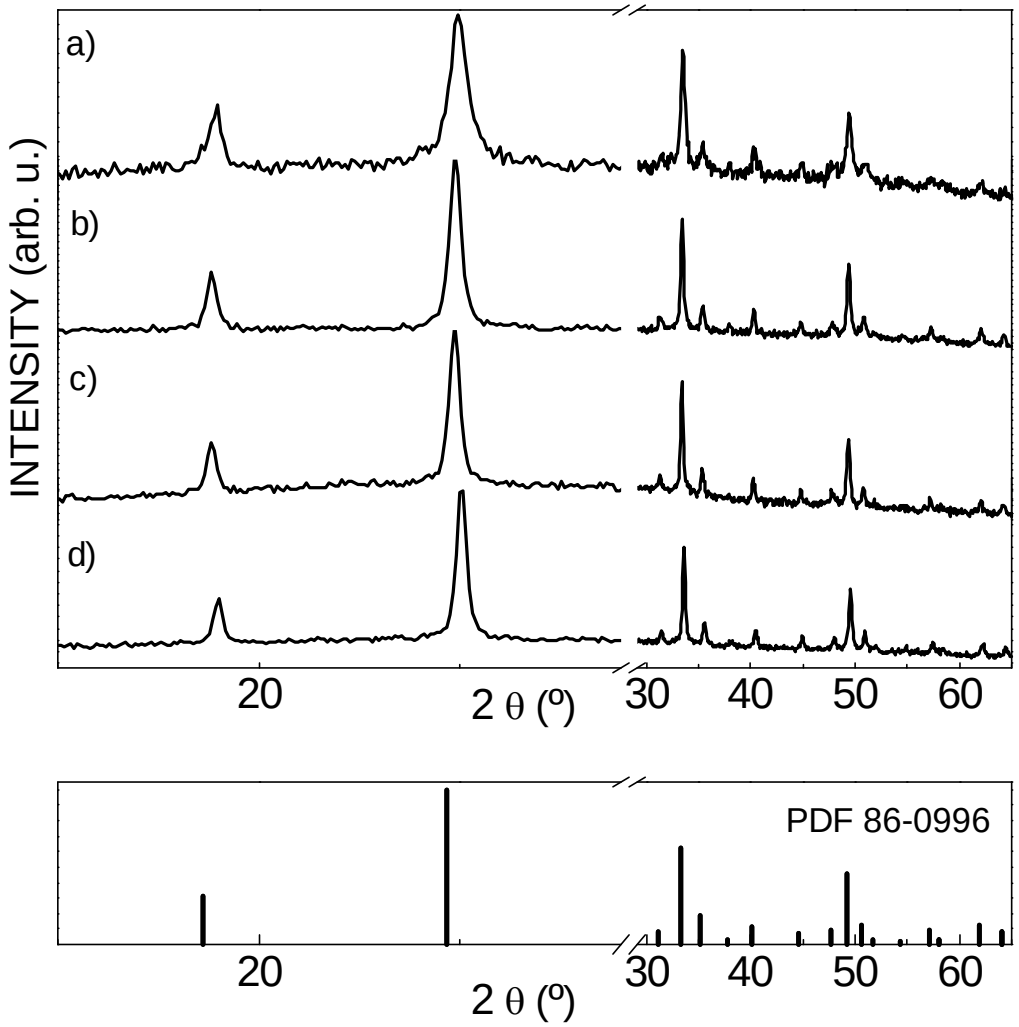

Figure S1. XRD patterns of $Gd_{0.995}Tm_{0.005}VO_4$ prepared by HT synthesis at 185 ºC using Gd and Tm nitrates with pH 7 and different reaction time *t*: a) *t*=2 ½ h, b) *t*=7 h, c) *t*=12 h and d) *t*=24 h. At the bottom, the XRD pattern scheme of tetragonal $I4_1/amd$ $GdVO_4$, JCPDS File 86-0996 is shown.

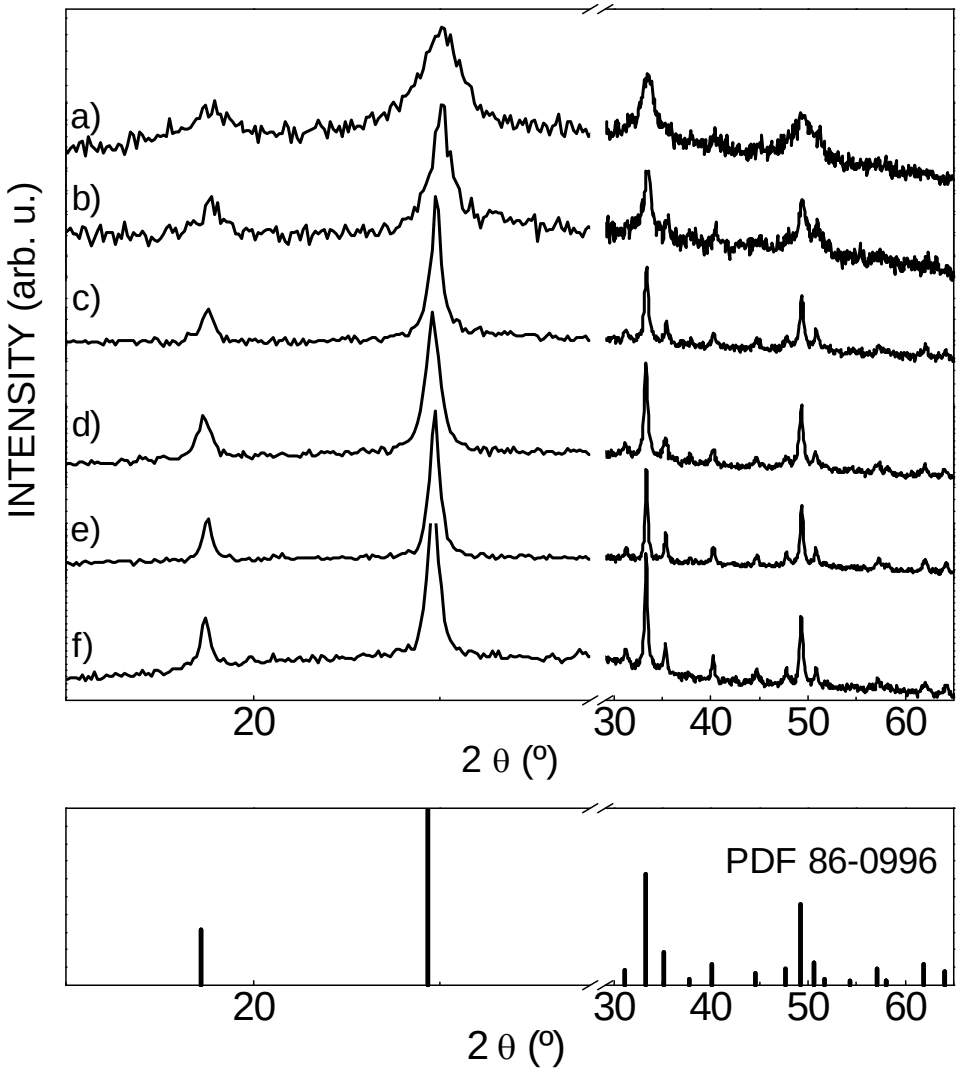

Figure S2. XRD patterns of $Gd_{0.95}Tm_{0.05}VO_4$ prepared by HT synthesis at 185 ºC using Gd and Tm chlorides with pH 4 and different periods of prior stirring and/or HT treatment: a) 24 h stirring; b) 1 h stirring, HT *t*= 1 h; c) 1 h stirring, HT *t*= 2 ½ h; d) HT *t*= 7 h; e) HT *t*= 12 h; f) HT *t*= 24 h. At the bottom, the XRD pattern scheme of tetragonal $I4_1/amd$ $GdVO_4$, JCPDS File 86-0996 is shown.

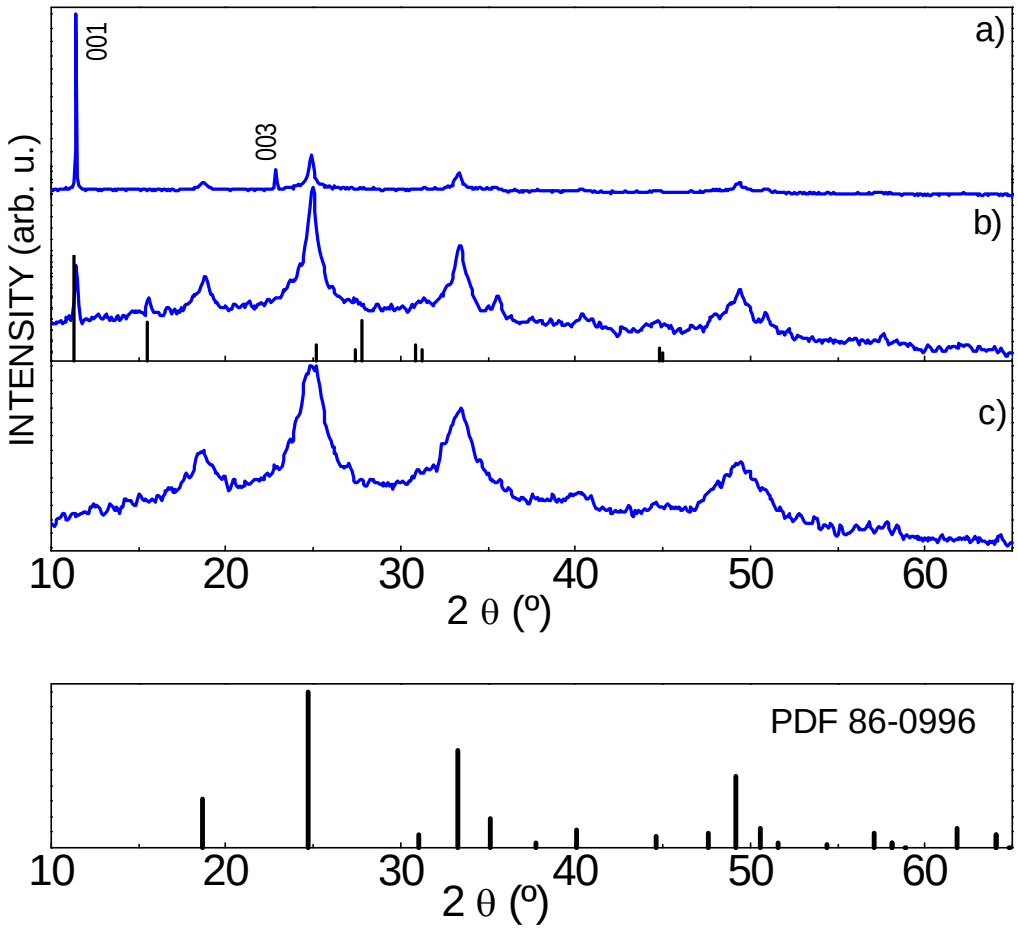

Figure S3. XRD patterns for prepared $Gd_{0.95}Tm_{0.05}VO_4$ using Gd and Tm nitrates in pH 4 medium and different periods of prior magnetic stirring and/or HT treatment: a) HT *t*=1 h, the sharp peaks have been indexed as (00*l*) reflections of a layered xerogel-like $V_2O_5.nH_2O$ phase; b) 1 h of stirring and HT *t*= 1 h, the vertical marks correspond to the scheme of Bragg peaks of the monoclinic layered NH_4VO_x phase; c) 24 h of magnetic stirring. At the bottom, the XRD pattern scheme of tetragonal $I4_1/amd$ $GdVO_4$, JCPDS File 86-0996 is shown.

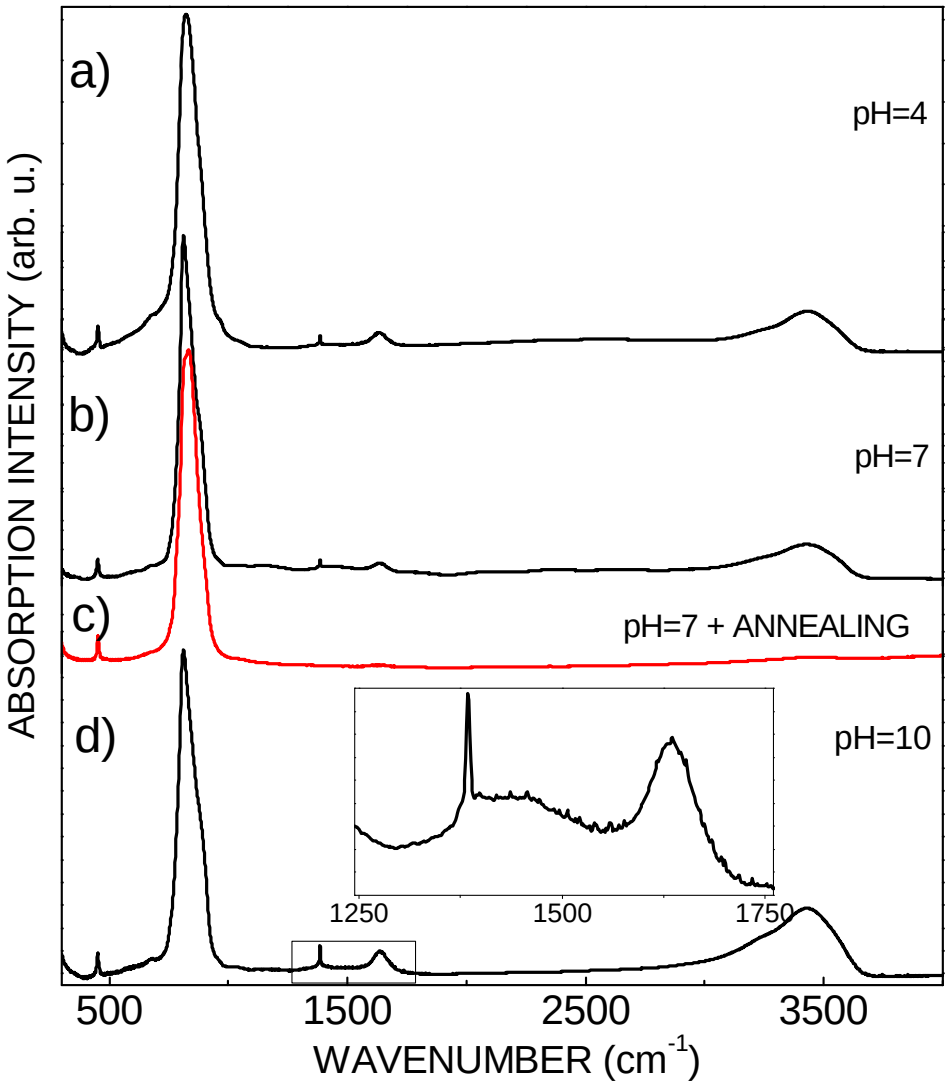

Figure S4. Room temperature FT IR spectra of $Gd_{0.95}Tm_{0.05}VO_4$ prepared by HT synthesis at 185 ºC using Gd and Tm nitrates and different pH medium: a) Acid, b) and c) neutral and d) and highly alkaline. Spectra in a), b) and d) are for as-prepared samples, and the spectrum in c) is for the pH 7 material 5 h annealed to 600 ºC.

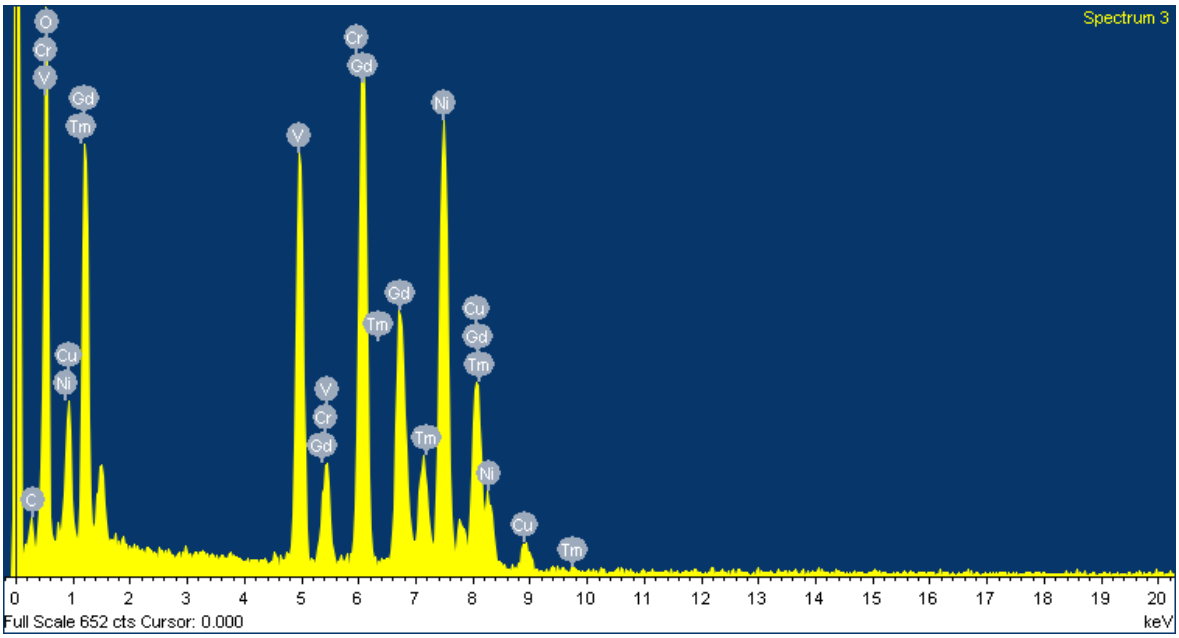

Figure S5. Energy dispersive X-ray spectrum for the sample in Figure 10, which indicates that Gd, V and Tm are in the atomic ratio 1:1:0.10, in agreement with the nominal composition, and the rest of peaks originate from the used grid.

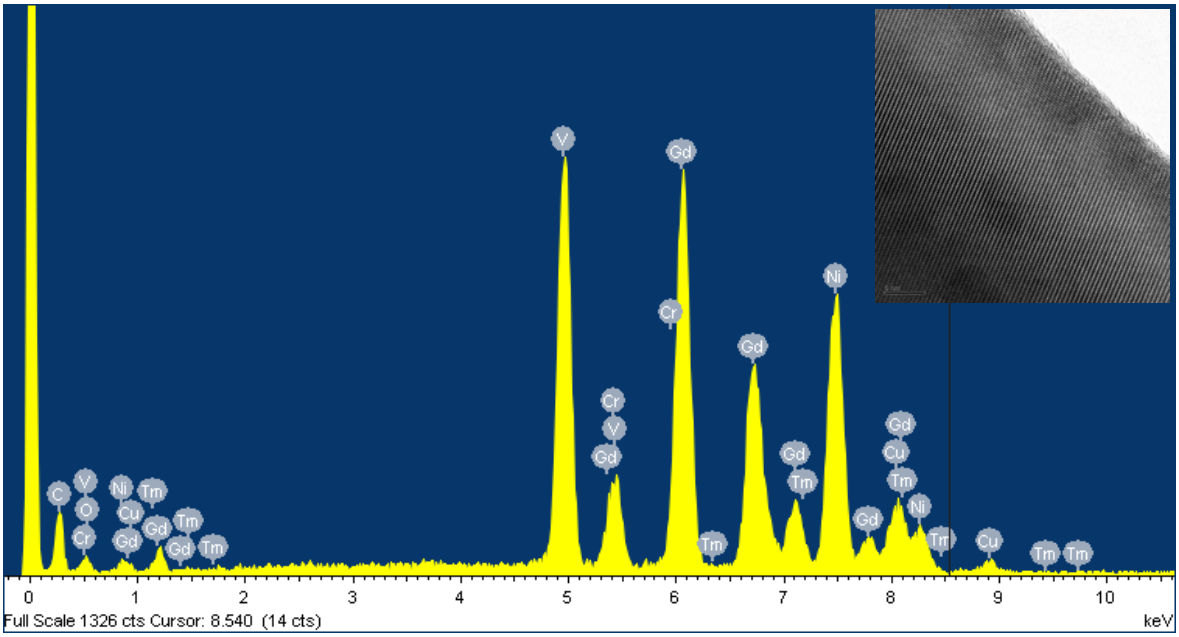

Figure S6. Energy dispersive X-ray spectrum for the sample in Figure 12, with peaks different from these of Gd, V and Tm originated from the used grid.

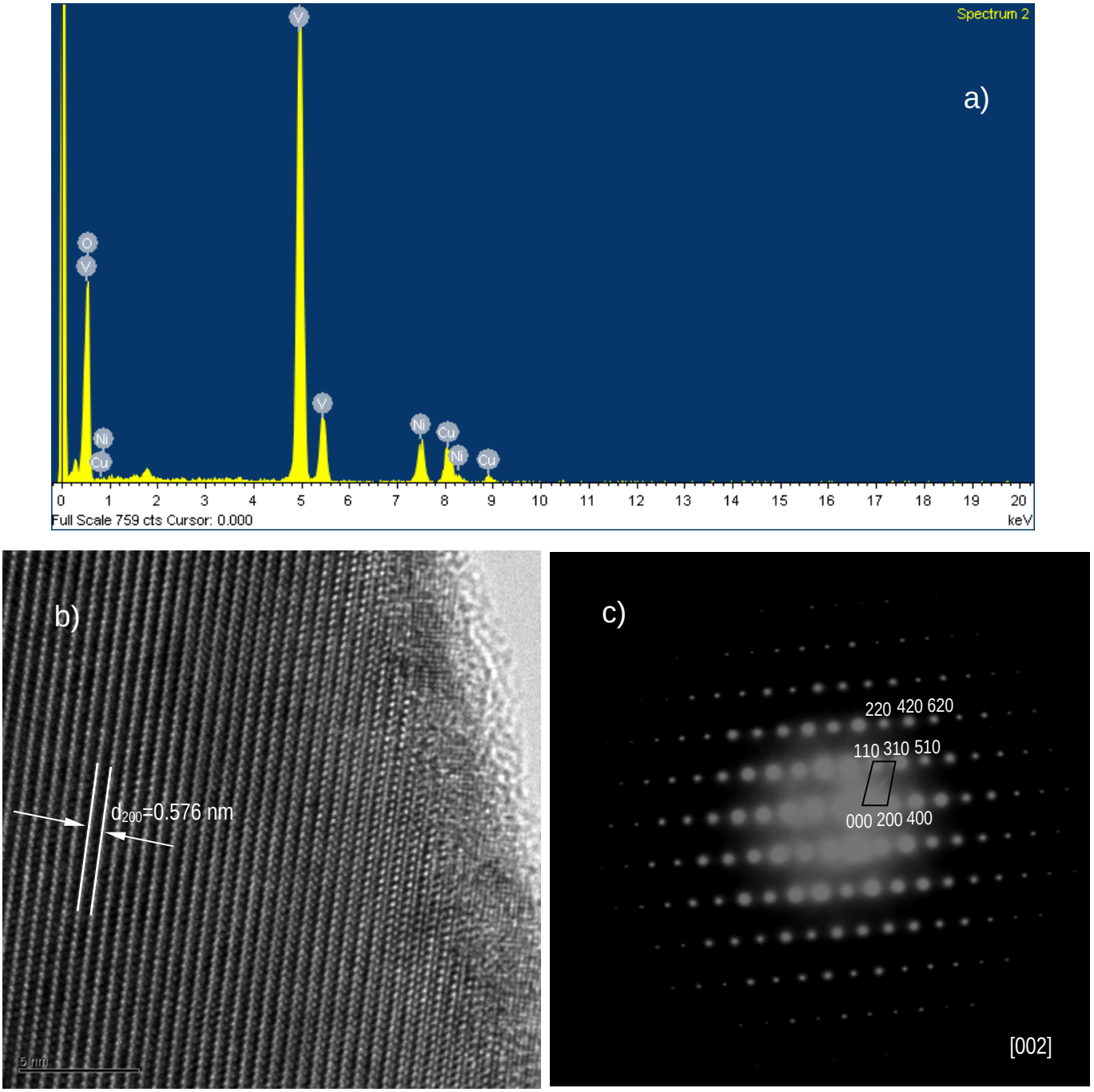

Figure S7. a) Energy dispersive X-ray spectrum for a V_2O_5 nanobelt (orthorhombic JCPDS File 89-0612), with peaks different from these of V originated from the used grid; b) and c) HRTEM image and indexed SAED pattern (along the [002] zone axis), respectively, of the V_2O_5 nanobelt.

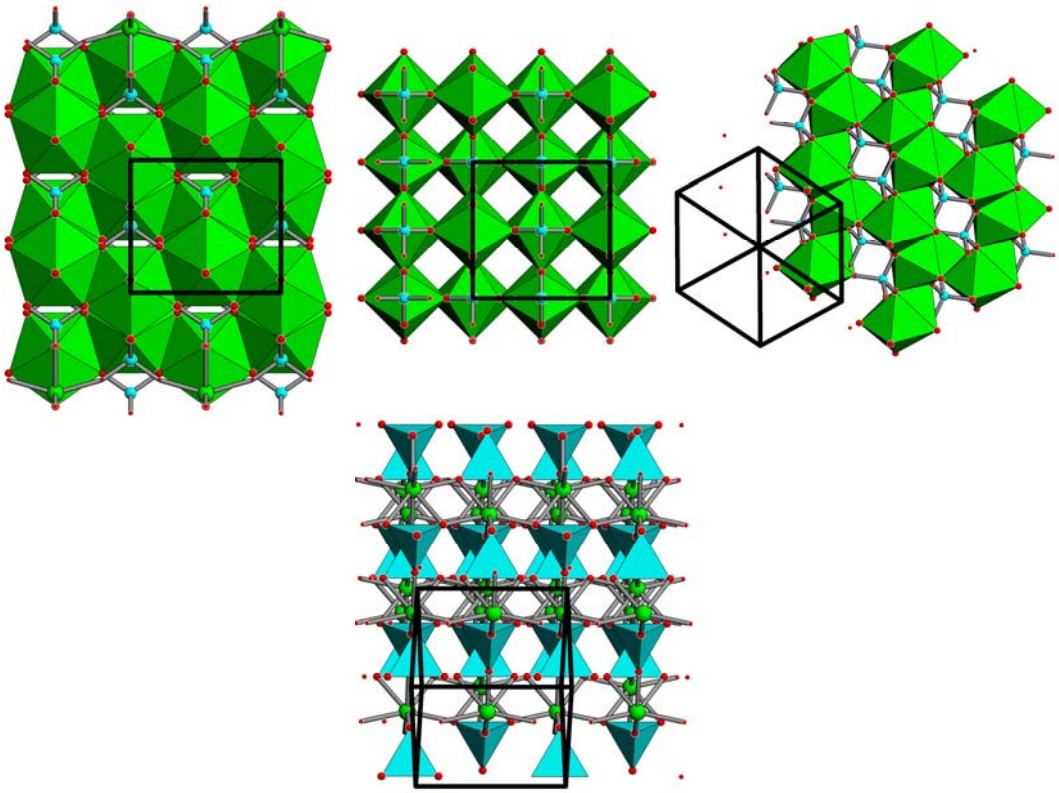

Figure S8. Description of the tetragonal $I4_1/amd$ zircon-type structure of $GdVO_4$: a), b) and c) GdO_8 dodecahedra (in green) share edges with each other forming chains parallel to the *a* axis, and each GdO_8 shares edges with four adjacent GdO_8 polyhedra, two in each of the equivalent directions [100] and [010]; The chains along *a* are cross-linked by sharing corners with VO_4 tetrahedra (in blue); Alternating GdO_8 and VO_4 also form edge-sharing chains parallel to *c*. The Figure S8d shows a view of $GdVO_4$ nearly aligned along the [101] vector, in which isolated VO_4 are organised in such a way that they seem a kind of layered structure, with GdO_8 polyhedra between VO_4 "layers". Green, blue and red spheres represent Gd, V and O, respectively.

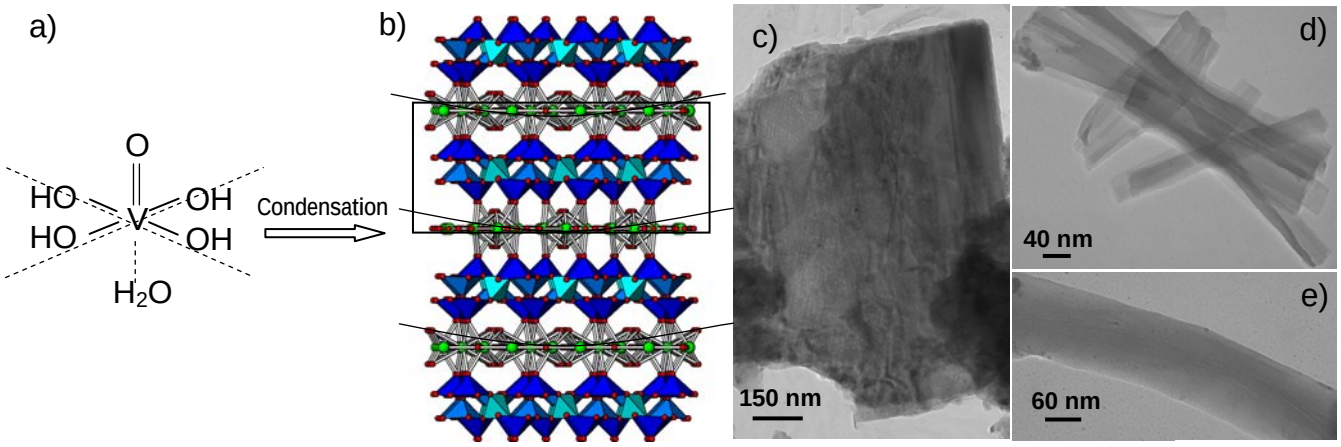

Figure S9. Illustration of the mechanism leading to the formation of tubular-like morphologies for HT $Gd_{1-x}Tm_xVO_4$ prepared at pH 4-7: a) The molecular precursor $[VO(OH)_4(H_2O)]^-$, b) a layered structure resulting from the condensation of the above precursor, c) view of a nanosheet, d) partially scrolled forms, and e) flexible nanotube of $Gd_{1-x}Tm_xVO_4$ materials. The depicted layered structure corresponds to $BaV_7O_{16}{\cdot}n(H_2O)$.

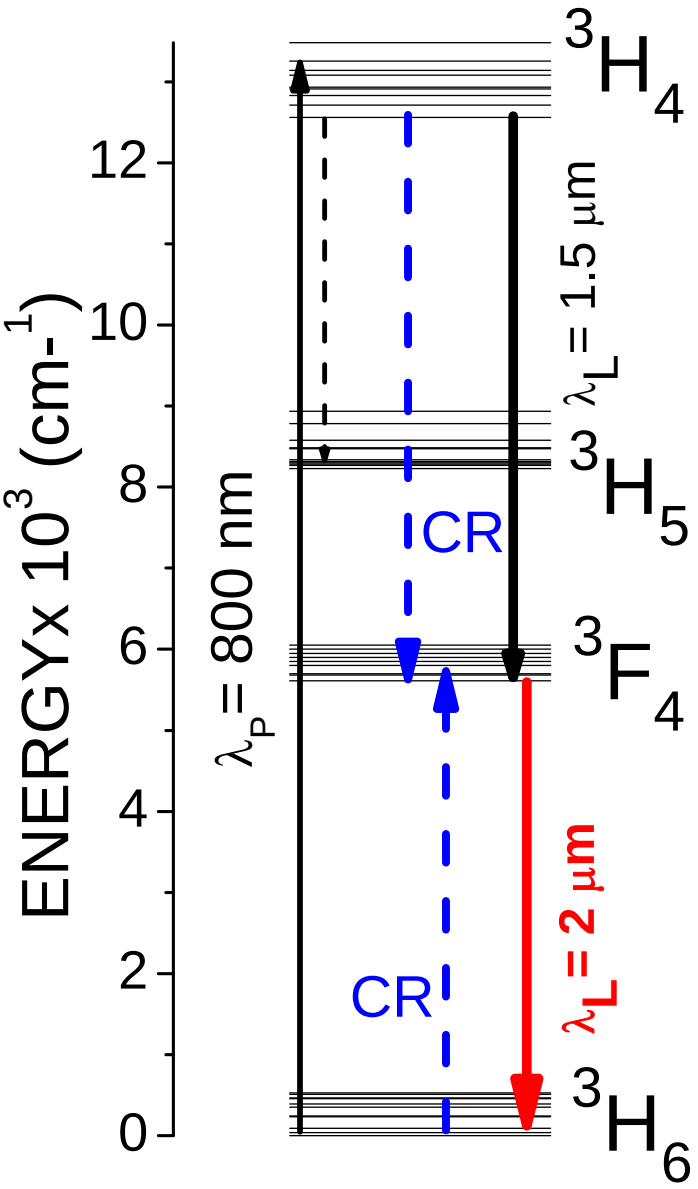

Figure S10. Scheme of energy levels of Tm^{3+}, showing relevant pumping and de-excitation paths for the $^3F_4 \rightarrow {}^3H_6$ laser emission operating at 1.8- 2.05 µm. Tm^{3+} ions can be efficiently excited around 800 nm through the ground state optical absorption of the $^3H_4$ multiplet. The laser multiplet $^3F_4$ is populated either by intraionic electron relaxation or by a cooperative cross-relaxation (CR) process that occurs through the interaction of two neighboring Tm^{3+} ions, $^3H_4 + {}^3H_6 \rightarrow 2\times{}^3F_4$. This laser channel can be directly and efficiently pumped with commercially available powerful semiconductor AlGaAs laser diodes around 800 nm, with little heat transfer to the crystal host.

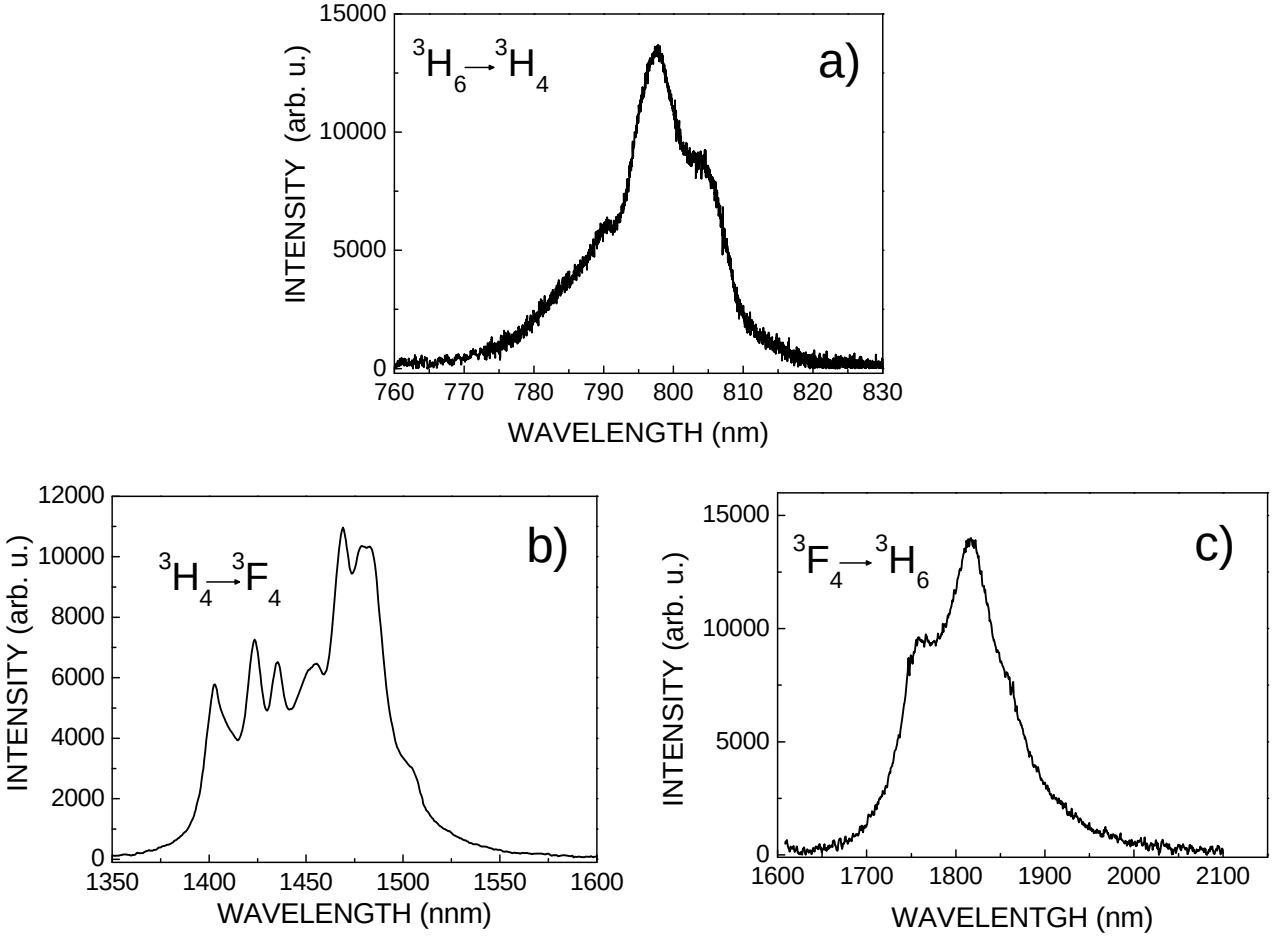

Figure S11. 300 K optical spectra for HT $Gd_{0.95}$ $Tm_{0.05}VO_4$ prepared at pH 4: a) Excitation spectrum (λ_{EMI}=1816 nm) of the $^3H_4$ multiplet; b) emission spectrum (λ_{EXC}=799.4 nm) of $^3H_4 \rightarrow {}^3F_4$; c) emission spectrum ($\lambda_{EXC}$=799.4 nm) of $^3F_4 \rightarrow {}^3H_6$.

Table S1. 300 K experimental lifetimes (τ, in μs) and intensities (I) of the $^3H_4$ photoluminescence of HT $Gd_{1-x}Tm_xVO_4$ products further annealed for 5 h to 600 ºC. PL decays were fit to $I(t)=I_1e^{-t/\tau1}+I_2e^{-t/\tau2}$ ($I_1+I_2=1$) curves. λ_{EXC}= 800 nm, λ_{EMI}= 1470 nm. Measurements carried out on samples dispersed in ethylene glycol.

pH 4																
	2 ½ h				6 h				13 h				24 h			
%Tm	I_1	τ_1	I_2/I	τ_2/τ	I_1	τ_1	I_2/I	τ_2/τ	I_1	τ_1	I_2/I	τ_2/τ	I_1	τ_1	I_2/I	τ_2/τ
0.2	-	-	1	137	-	-	1	127	-	-	1	130	-	-	1	144
0.5	-	-	1	126	-	-	1	120	-	-	1	129	-	-	1	124
1	0.25	20	0.75	90	-	-	1	83	0.31	30	0.69	81	-	-	1	85
5	0.47	4	0.53	12	0.44	3	0.56	16	0.40	6	0.60	12	0.85	6	0.15	15
pH 7																
	2 ½ h				6 h				13 h				24 h			
%Tm	I_1	τ_1	I_2/I	τ_2/τ	I_1	τ_1	I_2/I	τ_2/τ	I_1	τ_1	I_2	τ_2	I_1	τ_1	I_2	τ_2
0.2	-	-	1	143	-	-	1	155	0.15	30	0.85	133	0.20	40	0.80	154
0.5	-	-	1	120	0.11	20	0.89	120	0.08	30	0.92	130	0.24	30	0.76	120
1	0.14	10	0.86	89	0.17	20	0.83	100	0.30	30	0.70	110	0.27	40	0.73	115
5	0.78	6	0.22	30	0.72	6	0.28	46	0.67	5	0.33	40	0.60	5	0.40	35
pH 10																
	2 ½ h				6 h				13 h				24 h			
%Tm	I_1	τ_1	I_2	τ_2	I_1	τ_1	I_2/I	τ_2/τ	I_1	τ_1	I_2	τ_2	I_1	τ_1	I_2/I	τ_2/τ
0.2	0.41	50	0.59	140	-	-	1	129	0.34	40	0.66	142	-	-	1	126
0.5	0.35	30	0.65	109	0.45	40	0.55	124	0.25	30	0.57	114	0.20	20	0.80	110
1	0.54	30	0.46	98	0.50	20	0.50	84	0.43	20	0.57	82	0.48	28	0.52	85
5	0.60	3	0.40	10	0.66	3	0.34	11	0.64	3	0.36	12	0.64	2.7	0.36	14

Table S2. 300 K Experimental lifetimes (τ, in μs) and intensities (I) of the $^3F_4$ photoluminescence of HT $Gd_{1-x}Tm_xVO_4$ products further annealed for 5 h to 600 ºC. PL decays were fit to $I(t)=I_1e^{-t/\tau1}+I_2e^{-t/\tau2}$ ($I_1+I_2=1$) curves. λ_{EXC}= 800 nm, λ_{EMI}= 1816 nm. Measurements carried out on samples dispersed in ethylene glycol.

pH 4																
	2 ½ h				6 h				13 h				24 h			
% at Tm			I	τ	I_1	τ_1	I_2/I	τ_2/τ			I	τ			I	τ
0.2			1	690			1	735			NA	NA			1	800
0.5			1	699	0.57	410	0.43	729			1	619			1	710
1			1	272			1	353			1	418			1	333
5			1	36			1	79			1	35			1	40
pH 7																
	2 ½ h				6 h				13 h				24 h			
%Tm	I_1	τ_1	I_2/I	τ_2/τ	I_1	τ_1	I_2/I	τ_2/τ	I_1	τ_1	I_2/I	τ_2	I_1	τ_1	I_2/I	τ_2/τ
0.2			1	650			1	990			1	750			1	863
0.5	0.63	430	0.37	980			1	599			1	693			1	490
1			1	300			1	362	0.75	360	0.25	570			1	460
5	0.89	40	0.11	160	0.88	30	0.22	136	0.81	30	0.19	137	0.87	33	0.13	170
pH 10																
	2 ½ h				6 h				13 h				24 h			
%Tm	I_1	τ_1	I_2/I	τ_2/τ	I_1	τ_1	I_2/I	τ_2/τ	I_1	τ_1	I_2/I	τ_2/τ			I	τ
0.2			1	555			1	632			1	651			1	673
0.5	0.71	250	0.29	570	0.72	320	0.28	600	0.73	410	0.27	580			1	348
1	0.64	100	0.26	220	0.68	60	0.32	230			1	294			1	241
5			1	21			1	21			1	24			1	25